Identifying mechanisms responsible for misties between the synthetic seismogram and seismic data

Macdennis Nwaeze

December 2022

Table of content

I. <u>Introduction</u>

A. Well tie

Sheriff (1973) defined a *well tie* as “running a seismic line by a well so that seismic events may be correlated with subsurface information”. This correlation is accomplished by creating a synthetic seismogram from the logged sonic and density curves. Accurate well ties are essential for seismic inversion, which leads to a quantitative characterization of the reservoir.

Unfortunately, interpreters have observed poor synthetic ties since the early days of synthetics in the mid-1950s (White and Hu, 1998; Anderson and Newrick, 2008). Figure 1 contains an example of a poor well tie from the Delaware Basin. Of the many reasons for misties, both attenuation and internal multiples have been suspected since early studies by Ricker (1953) and McDonal et al. (1961). They showed that intrinsic attenuation affects the quality of the seismic data by producing a time-varying wavelet and this time-varying mechanism reduces the correlation of a well-tie. Theoretical examples of intrinsic attenuation were included in synthetics generated by Trorey (1962). He defined a time-varying wavelet with an explicit equation for absorption as a function of time rather than extracting it from well data.

A stationary wavelet w(t) was used by Wuenschel (1960) when he computed all internal multiples by defining the upgoing and downgoing wavefields at each boundary for normal incident (NI) plane waves. The wavelet, however, broaden as a function of time, but not due to intrinsic attenuation but by scattering attenuation. In 1971, O’Doherty and Anstey published the article *Reflections on Amplitudes* that contrasted the transitional versus cyclic sedimentary depositions. During cyclic depositions, they pointed out that "… primary reflection paths did not exist; the useful seismic information is carried be the very-short-delay multiple reflections". Using a ray-tracing approach, Schoenberger and Levin (1974) illustrated the broadening of the propagating wavelet with time due to stratigraphic filtering (also an attenuation mechanism). The separation of short-period multiples from long-period multiples was advanced with the work of Hubral et al. (1980). Starting with Hubral's concept of generalized primaries (similar in meaning to propagating wavelets), practical methods for separating short- from long-period multiples were published in a series of articles by Qi and Hilterman (2013-2018). Generalized primaries lead to numerous techniques to identify seismic multiples, especially when control well is available for proof of concept.

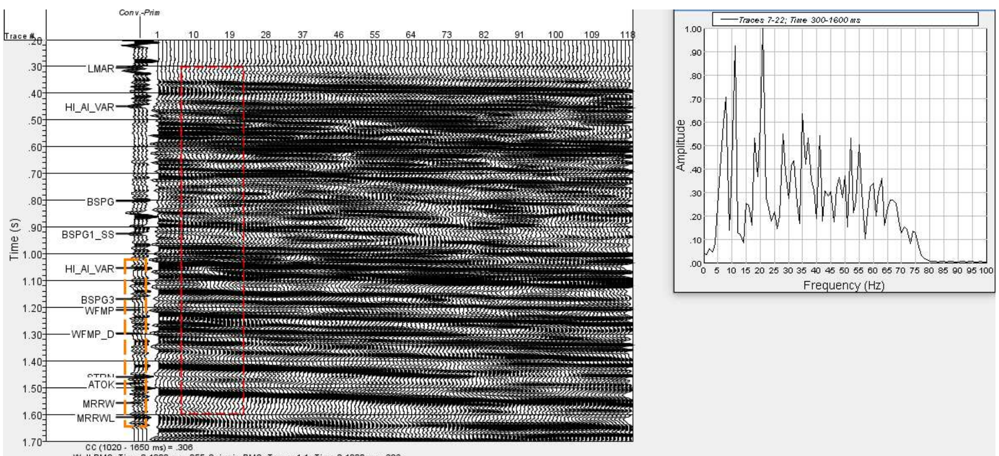

Figure 1. Typical Delaware basin 3D inline section, synthetic tie with primary-only events, and amplitude spectrum of traces within the red triangle.

II. **Statement of problem and initial objective**

In order to correct a synthetic mistie, the theoretical or physical cause of the mistie needs to be identified. Most of the time, the mechanism responsible for a mistie is related to multiples, and significant research has been conducted to remove the effects of multiples to improve the seismic well tie. Along this line, Hubral (1983) defined generalized primaries that incorporate both long-and short-period multiples in the propagating. Hubral's work provided a breakthrough in identifying the cause of internal multiples in seismic data and more importantly, assisted in identifying internal multiples and their acoustic impedance generators.

Of course, there are other reasons for misties other than multiples and Figure 2 lists other reasons for misties. The list is divided into catalogs that represent seismic, well-log quality, and theoretical problems. The figure implies the necessity of investigating the various catalogs that are required in the generation and interpretation of the seismic image. As mentioned, one of the main causes of misties is multiples that degrade the quality of the seismic data by creating extra events and producing a time-varying propagation wavelet. This propagating wavelet broadens and decreases in amplitude with increasing distance traveled. In essence, it has similar effects as that of intrinsic attenuation, which of course reduces the correlation of the well tie (Ricker, 1953; McDonal et al., 1961).

In this capstone project, I identified various reasons for misties in order to improve a well tie. Much of my effort has involved the interpretation problems that multiples create in seismic data. The final goal was to suggest alternate workflows that can be applied to identify the cause of the misties when multiples are suspected. Several examples are taken from published literature and where possible actual field data validated a specific workflow. As an example, amplitude variation with offset has led to misties that are often overlooked by the interpreter.

Seismic
- Data quality
- Well or seismic location is incorrect
- 2D sideswipe
- Tie synthetic to events > 12-trace continuity
- Tie synthetic to near-trace stack
- Tie 2D AVO synthetic stack to seismic stack

Model
- Check shot – review large drift corrections
- Deviation survey applied
- Improper amplitude or phase spectra
- Tie resistivity synthetics
- Compute AVO stacks
- Tie (Primary+Multiple) synthetics
- Wrong theoretical model
- Need attenuation mechanisms

Well-Log Curves
- Sonic and density logs don't correlate
- Sonic cycle skips removed
- Sonic and density values tie regional trends
- Caliper and tension curves are flat
- Invaded hydrocarbon zones
- Shallow sonic and density curves are questionable
- Sand and shale are affected differently by hole conditions
- Pseudo sonic and/or density logs needed
- Integrated sonic (20 kHz) is faster than seismic survey(60Hz) ?

Figure 2. Possible reasons for poor well ties (Hilterman, 2001)

III. Background of study area and technology

Datasets from two different locales were used in this project, the first dataset was from the Delaware Basin, and the second set from Cooper Basin, Australia. The stratigraphy in the Delaware Basin contains numerous beds of evaporites that are cyclically stratified in the shallow earth section, and they have large acoustic-impedance contrasts. These contrasts generate internal multiples and lower the frequency of the propagating wavelet. Figure 3 shows the location and stratigraphic section for the Delaware Basin datasets.

The second dataset was the Togar 3D seismic survey (Cooper Basin, Queensland Australia), which has range-limited pre-stacks migrations (0-600m and 1200-1800m) along with numerous suites of well-log curves.

TIPs well log modeler, a HSB Geophysical product, was used in conducting this study. The package includes software for (1) well-log editing, (2) modeling of 1D and AVO synthetics, wedge models, (3) building rock-physics templates for seismic attributes, and (4) processing software to identify and suppress multiples.

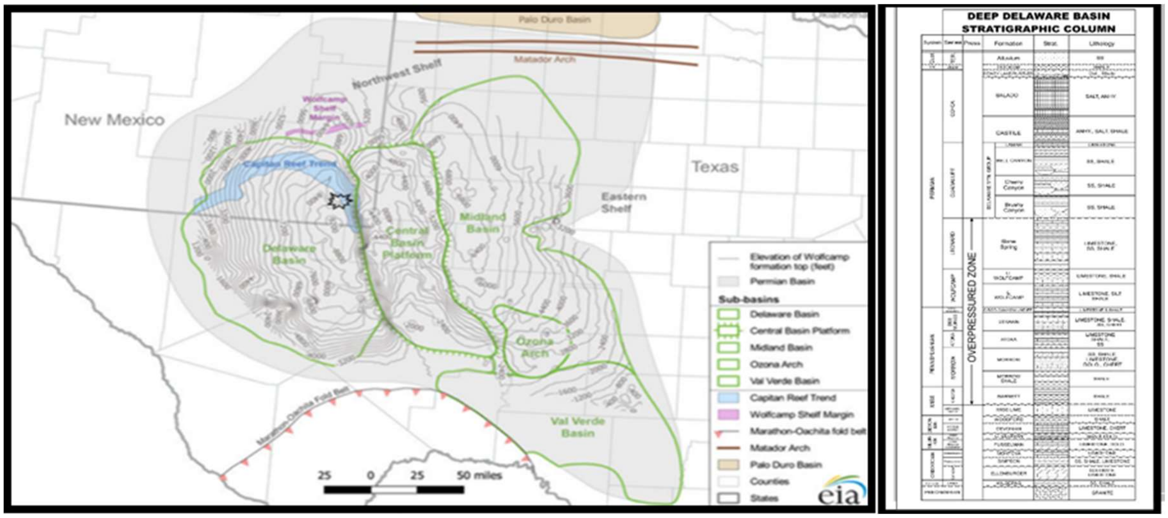

Figure 3. Stratigraphic chart and well location in the Delaware Basin portion of the Permian Basin (U.S. Energy Information Administration based on Enverus Drilling Info Inc., U.S. Geological Survey).

IV. Theory of internal multiples

Seismic well ties normally involve creating a 1D normal-incident (NI) synthetic seismogram where the seismic wavelet is stationary (not time varying). Mathematically, the 1D synthetic is expressed as s(t)=w(t)*r(t); where, s(t)= synthetic, w(t)=wavelet, r(t)=earth reflectivity, and * is the convolution operator. The reflectivity in this mathematical model is assumed to contain primary events only. This mathematical model is extended to include time-varying wavelets and multiple events. The multiple events are normally divided into short- and long-period multiples as illustrated in Figure 4. For land acquisition surveys, surface-related multiples are normally ignored.

Obviously, long- and short-period internal multiples degrade the correlation of a well tie. Long-period internal multiples reduce the quality of the seismic data by creating new events, and short-period internal multiples delay and distort the propagating wavelet similar to the effects of intrinsic attenuation (Figure 4). These mechanisms are prevalent in areas with numerous thin beds with high-contrast impedance layers, cyclically stratified such as the west Texas Delaware

Basin evaporite sequence and the Permian-aged coal beds in Cooper Basin, Queensland, Australia.

Numerous theories have been suggested on how to quantify internal multiples by incorporating them into the synthetic seismogram. Goupillaud (1961) presented the 1D earth model (Figure 5a) to account for all NI primary and multiple paths. Trorey 1962 presented an alternate method to model seismograms with frequency and depth dependent attenuation. O'Doherty and Anstey (1971) described the transmission of a source spike as it travels through numerous high-contrast layers such as the evaporite beds, sketched in Figure 5b. The transmitted impulse response is a time series with relative weights of 1, rc^2, rc^4, … etc., where the weights are separated by the two-way traveltime in the thin bed. The convolution of these transmitted pulses with one another as they travel through the thin beds constitutes the signal portion of the transmitted wavelet, whose shape approaches that of a Gaussian wave.

Hubral's et al. (1980) definition of the generalized primary incorporated long-and short-period internal multiples into the propagating wavelet and led to the quantification of internal multiples that degrade the quality of a well tie. Hubral started with Goupillaud's concept of propagating energy through layers that had the same traveltime interval. He used matrices composed of the upgoing and downgoing wavefields at each interface to propagate energy. This allowed Hubral to arbitrarily stop the propagation at a specific interface and examine the wavefields. With this procedure, the propagating wavelet at every time sample in the reflectivity function of the earth can be defined. Now the primary-only reflectivity is convolved with the "wavelet array" which is defined as the matrix of propagating wavelets, one wavelet for each time sample. This is a convolution of the reflectivity with a time-varying "wavelet". The synthetic generated by Hubral is exactly equal to the synthetic generated by Goupillaud's method. The significance of Hubral's method is that his propagating wavelet is composed of a short-period multiple plus a long-period multiple. They can be separated so that if the primary-only reflectivity is convolved with the "wavelet array" where only the short-period multiples of the propagating wavelet are included in the wavelet array, a primary-only synthetic will be generated with a time-varying wavelet. This is referred to as the stratigraphic filtered (SF) primary-only synthetic. The wavelet (more appropriately called the "wavelet array") is time variant as it represents the scattering attenuation at the well site. In a similar fashion, the multiple portion of the propagating wavelets can be selected so that after convolution with the primary reflectivity the SF multiple-only synthetic is generated.

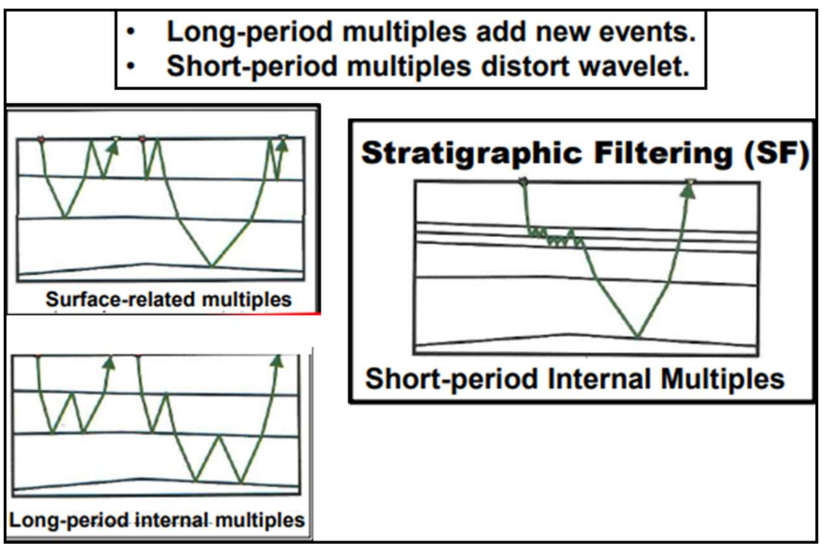

Figure 4. Internal multiples degrade the quality of seismic data and the synthetic seismogram (modified from Hilterman F. J, Seismic Amplitude Interpretation Course Notes, 2022).

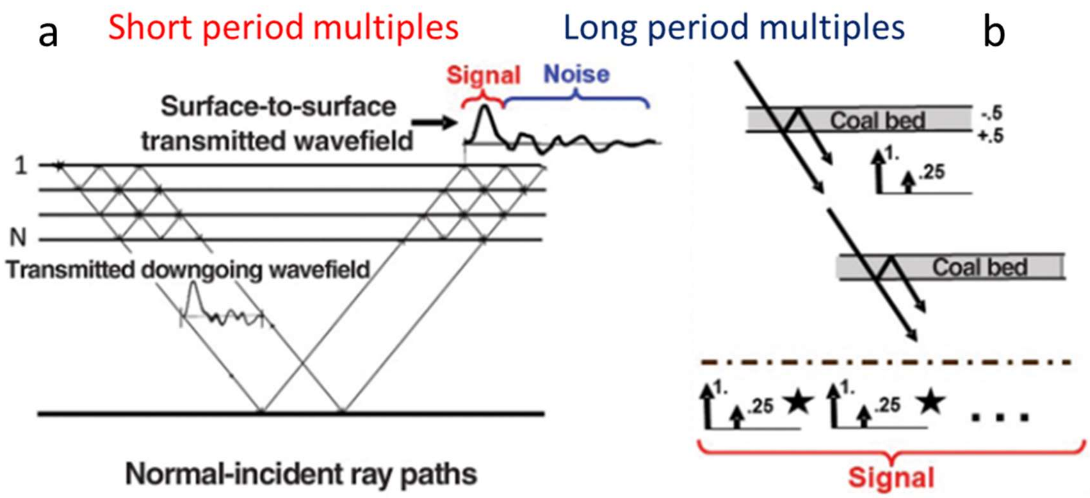

Figure 5. Earth model for generation of multiple synthetics. (a) Equal time interval model representing all normal-incident ray paths for deep two-way transmitted wavelet. (b) Convolution model for thin-bed transmitted wavelets through multilayers. (Hilterman et al, 2018).

V. Multiple identification

Figure 6 shows well logs from the Delaware Basin, in West Texas where the near surface contains thin beds of limestone, anhydrite and salt, that lead to large changes in acoustic impedance. This cyclic stratification of evaporite beds leads to the generation of both long-period and short-period multiples The short-period multiples will distort the propagating wavelet while the long-period multiples can possibly overlap the primary reflections in the hydrocarbon zone of interest (ZOI) from 6,000-16,000 ft depth.

The four synthetics generated from the propagating wavelet catalog are displayed in Figure 7 with the frequency bands of 2-4-80-120 Hz to 2-4-15-25 Hz. The Multiple + Primary synthetic in Figure 7 can be thought of as representing the seismic data. As such, this synthetic is normally tied to PSTM data to determine if internal multiples are significantly present in the PSTM data. If long-period multiples are interpreted to not exist, then the SF primary-only is tied to the PSTM data, and the SF multiple will have low amplitude compared to the SF primary-only. The effects of long-period multiples (SF multiples) are not as evident on the low-frequency synthetics and therefore filtering both seismic and primary synthetics to a lower frequency increases the well tie correlation. The effects of long-period internal multiples at various times in the synthetic can be observed by creating a new TD by cropping the well-log curves to a shallower depth. Only multiples are present below the new TD and thus the process of repeating the TD cropping leads to a method of identifying the source of multiples.

Using the same well log curves as those in Figures 6-7, a propagating wavelet panel was created and is shown in Figure 8. For this panel, a two-way propagating wavelet (PW) was computed for every time sample and a sub-set of the PW were plotted to constitute the wavelet dictionary shown. The impedance log is displayed as a function of time. Figure 8a had a spike as the source, while Figure 8b had a zero-phase 2-4-50-60Hz source. The area of the wavelets with a blue background represents the short-period multiples and these are the wavelets that we associate with reflections off the boundaries. The portion of the PW with a red background are the long-period multiples and it is easy to see that the long-period multiples have a higher frequency band than the short-period multiples. From the panel, the transmitted wavelet broadens with depth with an increase in the noise coda (high frequency tail) as the high impedance contrast layers are traversed. The broadening of the short-period multiples is caused by scattering phenomenon, which is an effect of stratigraphic filtering (short-period internal multiples).

The propagating wavelets in Figure 8a are all minimum-phase while thus in Figure 8b are mixed phase since the source was zero phase. What is evident in Figure 8b is that the wavelet for time 50ms (far left wavelet) is a symmetric zero-phase wavelet that gradationally changes to a lower frequency with depth (time) so that at TD the short-period multiple appears to have a 90-degree phase shift. This means two deconvolutions in a cascade fashion are needed to correct the total trace to zero-phase. An inverse Q filter could approximately correct for the 90-degree phase shift.

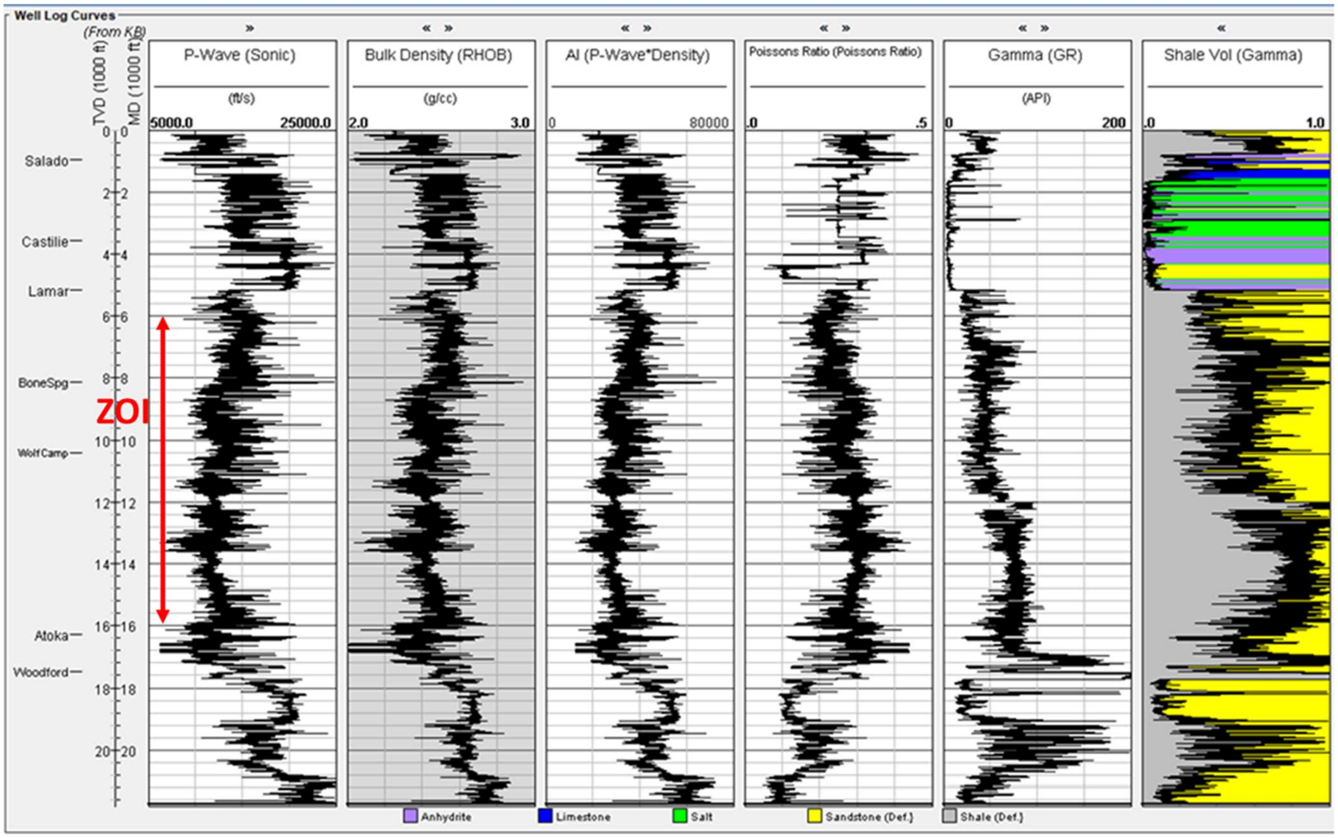

Figure 6. Well-log curves from the Delaware Basin showing the hydrocarbon zone of interest (ZOI).

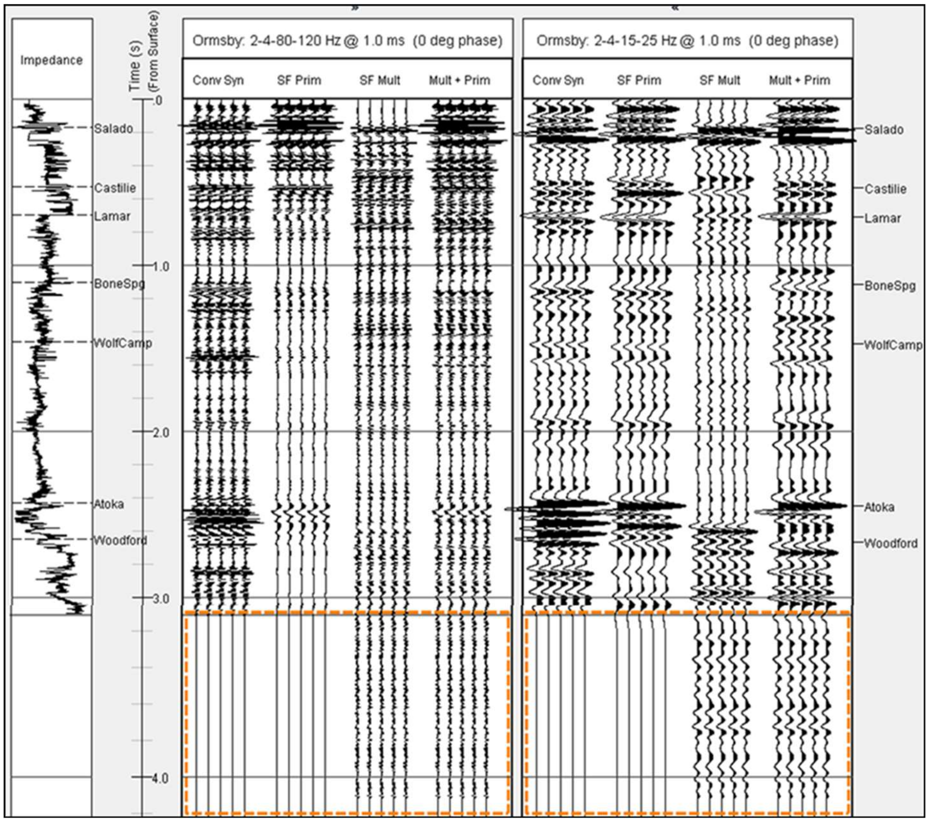

Figure 7. (a) Conventional primary-only, stratigraphic filter primary-only, stratigraphic filter multiples-only and stratigraphic filter primary + multiples synthetic seismograms generated with two different frequency bandwidths: Ormsby 2-4-80-120 Hz and an Ormsby 2-4-15-25 Hz wavelet, showing multiple events below TD (orange dashed box).

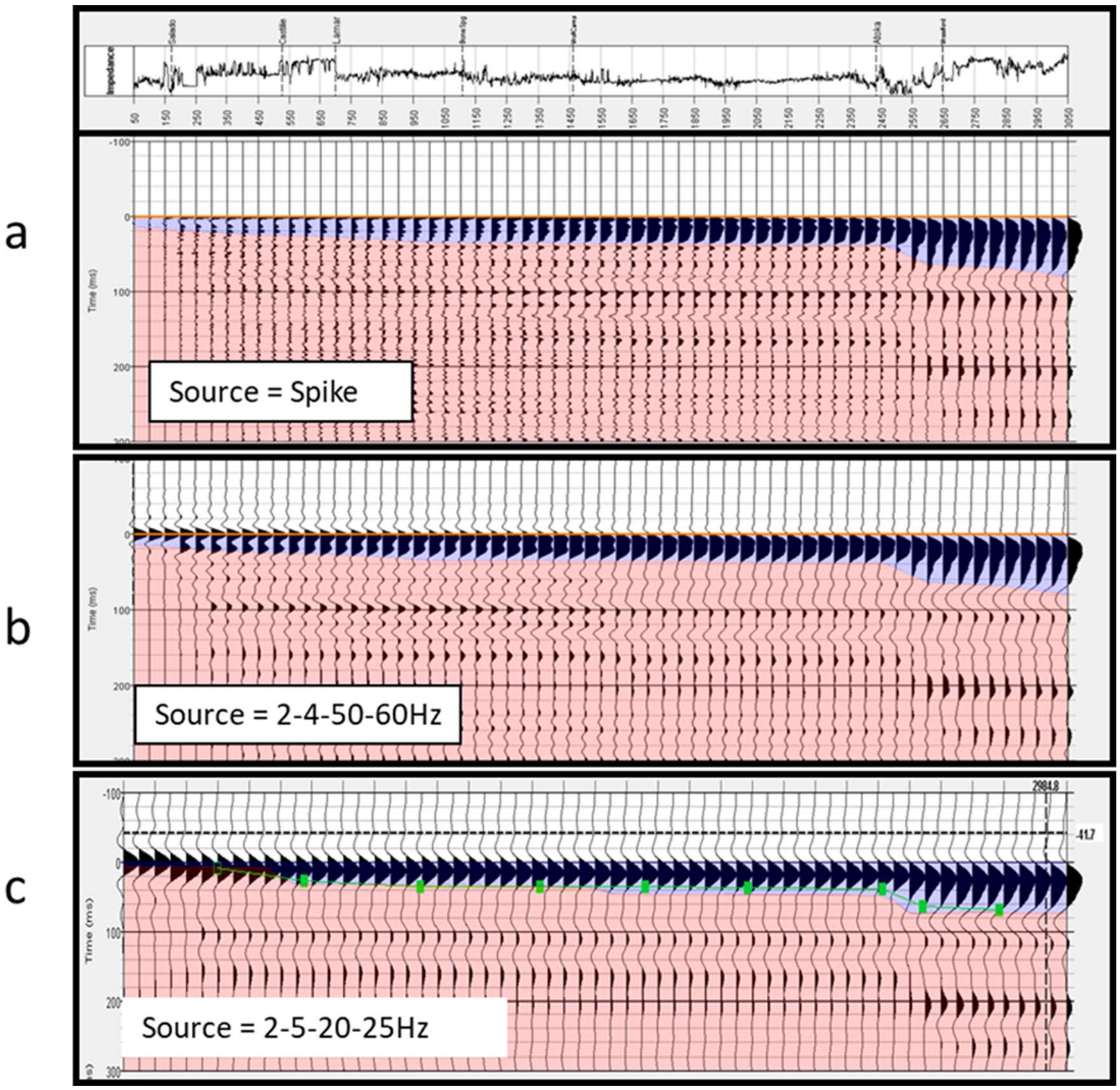

Figure 8. (a) Propagating wavelet panel with a spike source. The propagating wavelet changes from a spike to a gaussian pulse with high frequency reverberations. (b) Propagating wavelet panel with Ormsby 2-4-50-60 Hz source. (c) Propagating wavelet panel with a 2-5-20-25 Hz source

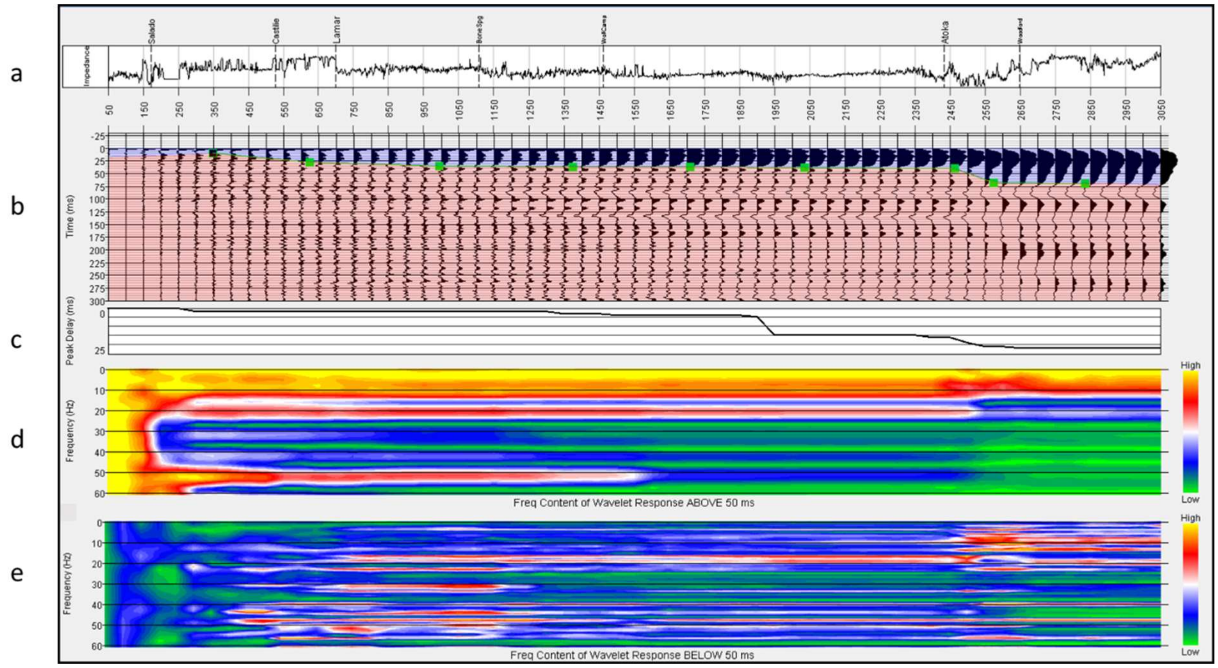

Figure 9; (a) Impedance log as a function of time. (b) Propagating wavelet panel with no filter applied. (c) Peak delay curve (ms). (d) Frequency spectra is based on the wavelet above 50 (ms). (e) Frequency spectra is based on the wavelet below 50ms.

A 2-4-50-60 Hz filter was applied to the propagating wavelet panel (Figure 8b), The high frequency reverberations are reduced, and the wavelets are more defined, improving continuity for defining multiple generators. In addition, there is a phase distortion, which is a minimum phase propagation effect. The phase distortion will affect processing and inversion interpretations beneath the evaporite beds. Finally, a 2-5-20-25 Hz source was applied to the wavelet panel (Figure 8c), suppressing the high frequency reverberations observed in Figures (8a and b) .The source wavelet applied at Figure 8c is an indication of the maximum frequency band that can be applied to both the seismic and synthetic seismogram to quell the effects of long-period internal multiple.

Additionally, the frequency spectra were generated for the first 50ms of the propagating wavelet (Figure 9d) and for 50-300 ms of the propagating wavelet panel (Figure 9e). Figures 9d and 9e illustrate the frequency variation as the wavelet transverse the evaporite beds. From

Figure 9d, it is observable that for the first 50ms of the propagating wavelets, the low frequency is enhanced and there is a considerable loss of high frequency. Beneath 50ms, which comprises of high frequency noise coda (long-period internal multiples), the low-frequency amplitude is reduced and depleted in the deeper portion of the impedance log and there is an apparent increase in magnitude of high frequencies. From the observed spectra and thin bed stratigraphy, transmission enhances the low frequency while reflection enhances high frequency. Figure 9 also shows the peak-delay plot generated from the propagating wavelet panel. The modelled propagating wavelet has a delay of 22 ms, making time on synthetic seismogram shorter than the seismic image by 22 ms. Possible interpretation workflows are listed that can be applied in areas prominent with internal multiples that are based on observations from the propagating wavelet catalog.

1) The horizontal orange line at time zero (Figure 8a) represents 2-way sonic adjusted traveltimes to which the individual propagating wavelets (PW) have been aligned. The difference between the peaks on the PW and the sonic time represent the stretch needed to effectively tie the seismic to the primary-only synthetic seismogram.
2) The peak delay time has been estimated to be 22 ms, from Stewart et al (1984) the Q (scattering) can be computed and then removed with inverse Q-filtering
3) Maximum frequency band with a high S/N was predicted to be 2-5-20-25 to suppress the high frequency tail of long-period multiples in the propagating wavelet dictionary (Figure 8c).
4) Long period multiples favor high frequency than the traversing short-period multiple wavelets.

5) Change in the shape and phase of the propagating wavelet prevents the use of a single deconvolution operator, therefore a cascade deconvolution needs to be applied at each timestep interval with a clear change in the shape of the signal for processing.
6) A. Fourier transform can be applied to the short period multiple to better estimate the low-pass filter for isolating primary events from multiples.
7) An estimate of a multiple generator time and its magnitude is possible by associating horizontal events starting left-most position and the time delay from short-period multiple start time.

Wedge model

A wedge model (Figure 10) is a synthetic section used to observe the seismic attributes and effects of internal multiples as a function of increasing model thickness. The wedge was set with the top at 6350 ft, directly below the large drop in acoustic impedance. Numerous thin beds of salt, anhydrite and limestone that have large acoustic impedance contrasts exists above the wedge top. This results in normal incident reflection magnitudes above the wedge to act as generators of internal multiples. The wedge model has an initial thickness of 200ft, with 31 increments of 10ft.

Figure 10 (i) contains primary-only wedge synthetics with Ormsby wavelets of 2-4-45-55 Hz (Figure 10 (i) (a)) and 2-5-20-25 Hz (Figure 10 (i)(b)). The high-pass Ormsby wavelet (Figure 10 (i) (a)) shows high-frequency reverberations, while the low-pass Ormsby (2-5-20-25 Hz) wedge model, has suppressed reverberations.

In Figure 10 (ii) internal multiples were applied with the same two frequency filters that were used in Figure 10. In this figure, all flat events below the top of the wedge are multiples with additional multiples dipping due to the wedge effect. As expected, multiples exist also exist above the wedge top but are difficult to diagnose (Figure 10 (ii)(a)). Figure 10 (ii)(b) has a low-pass Ormsby 2-5-20-25 Hz wavelet, which suppresses the long-period multiples below the wedge top improving the fidelity of the true wedge shape.

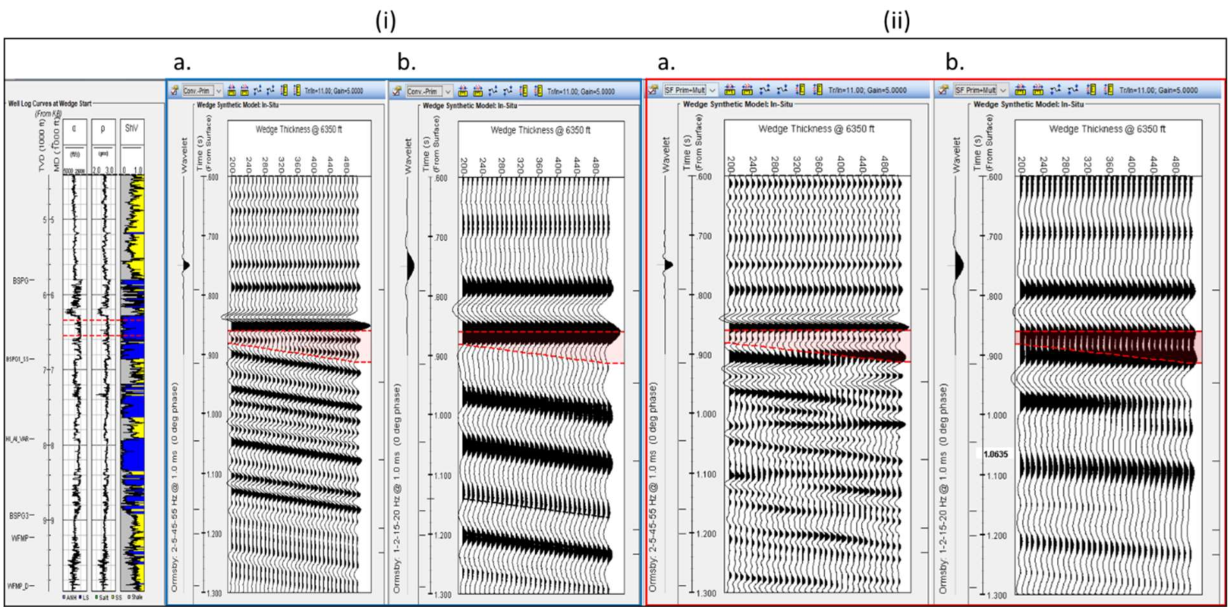

Figure 10 (i) Conventional primary- only wedge model generated with an Ormsby 2-4-45-55 Hz wavelet that corresponds to the frequency content of the Delaware basin seismic (a), (b) has a low- pass Ormsby 2-5-20-25 Hz wavelet.
Figure 10 (ii) The stratigraphic filtering effect from internal multiples is evident in both seismic panels in the figure. The primary + multiple synthetic generated with an Ormsby 2-4-45-55 Hz wavelet (Figure 10 (ii)(a)) that corresponds to the frequency content data content of the Delaware basin seismic line and a low- pass Ormsby 2-5-20-25 Hz wavelet (Figure 10 (ii)(b)).reduces the effect of the long-period multiples

VI. <u>Field examples</u>

A. Seismic well tie from Permian Basin West Texas

The quality of seismic data is a major contributor to the success of a well tie (Figure 11a). Figure 1 is the first attempt of a well tie in the Delaware Basin. The measure of the goodness-of-fit is the cross-correlation coefficient. The well tie has a low correlation coefficient of 0.306 and the seismic data contains numerous reflectors that show no coherency, and this should raise suspicion to the eye of the trained interpreter. The evaporite thin-bed sequences in the Delaware Basin present large acoustic impedance contrasts. As the propagating wavelet transverses through the thin beds, it maintains a minimum phase shape and becomes additionally distorted and transformed into a low-frequency bell-shaped wavelet. This minimum-phase low-frequency portion is at the front-end of the propagating wavelet is an effect of short-period multiples. The front-end of the propagating wavelet reflects off interfaces below it, giving the trace its low-frequency appearance. Meanwhile, the later portion of the propagating wavelet are long-period multiples and when they reflect off deeper interfaces, they generate new events, which are multiples. These multiples have a higher-frequency since their wavefields have been enhanced by the numerous times they reflect off thin-bed sequences as they propagate through their oscillating up-and-down path from source to receiver. The high- and low-frequency aspect of multiples was a major contribution described by O'Doherty and Anstey.

In Figure 11b, I applied a low pass 1-2-15-20 Hz filter to the seismic data of Figure 11a to enhance the low-frequency short-period multiples and suppress the long-period multiples of the propagating wavelet.

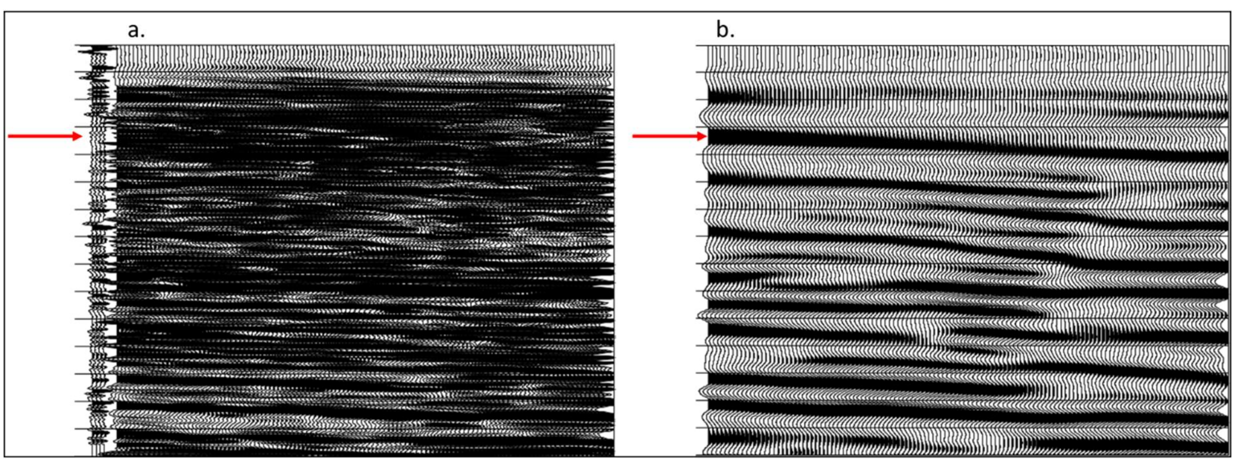

Figure 11, (a) Delaware basin seismic image. (b) Delaware basin section from with a low-pass 1-2-15-20 Hz filter applied.

The applied filter in Figure 11b corresponds to frequency spectra generated for the propagating signal (above 50ms) (Figure 9d). Although high frequency is lost which reduces the seismic resolution, the structural interpretation below the evaporite beds is totally different in Figure 11b than that in Figure 11a.

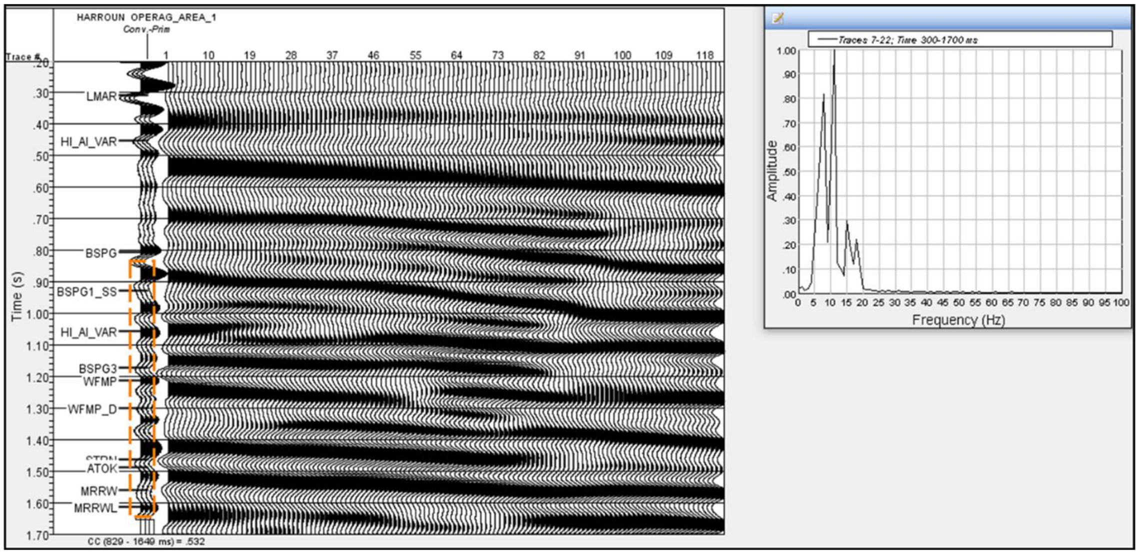

Figure 12. Delaware Basin well tie after a high-cut Ormsby 1-2-15-20 Hz filter was applied to both the seismic data and the conventional primary only synthetic seismogram.

Figure 12 shows the second well-tie attempt where an Ormsby 1-2-15-20 Hz filter was applied to both the seismic and synthetic. To preserve the integrity of the lithologic interpretation, I avoided stretching and/or squeezing the synthetic seismogram. The cross-correlation range was used to determine how well the synthetic seismogram tied the seismic and this value increased from 0.306 with the extracted wavelet primary only synthetic seismogram (Figure 11a) to 0.532 with the low-pass filter applied tied with a primary only synthetic seismogram.

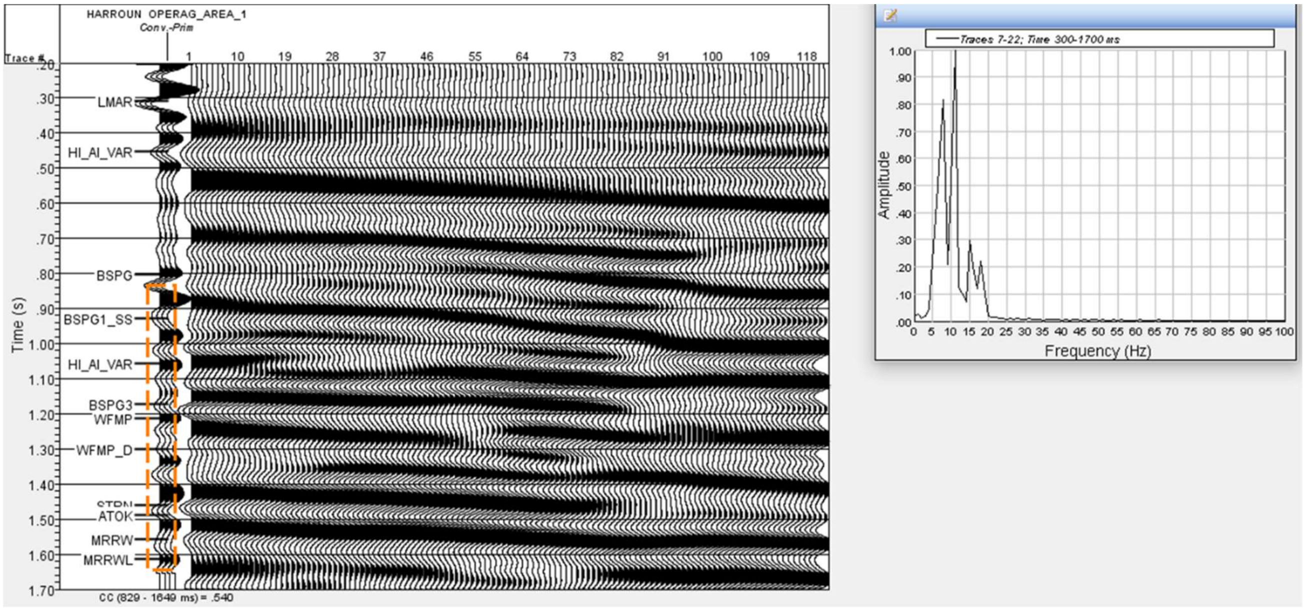

Figure 13. Delaware basin well tie with spectrum of extracted wavelet from the seismic data

Short period multiples (stratigraphic filtering) attenuated and delayed the propagating wavelet by 22 ms, meaning that the TD time on the synthetic seismogram is shorter than the real seismic data. The well tie with an extracted wavelet was used to compensate for the delaying effect and improved the correlation of the tie to 0.540 (Figure 13). Using an extracted wavelet from the seismic data in the creation of the synthetic seismogram enables filters to be designed to deblur the recorded seismic time series and allows the integration of "downhole" and surface seismic data for seismic interpretation purposes (Walden et al, 1998). However, the seismic data were not filtered with the same spectrum that the extracted wavelet had.

B. Seismic well tie from Cooper Basin

Amplitude variation with offset is also a mechanism that can reduce the correlation and degrade the well tie. Koefoed in 1955 presented observations that relates the shape of the AVO curve to changes in Poisson's ratio. This led Koefoed to suggest that lithology could be extracted from seismic data by estimating Poisson's ratio to identify the rock lithology. Along this line

Shuey (1985) presented a three-term approximation of Zoeppritz's equation. The Shuey AVO equation (Figure 14) incorporates the acoustic impedance, Poisson's ratio, and P-wave velocity to derive the reflection coefficient at the interpreter's choice of incidence angle. Shuey's AVO equation incorporated ideals from Koefoed observations in 1955 to correlate the changes in Poisson's ratio, a lithology indicator (Figure 14b), to the variations in amplitude with offset and incidence angle.

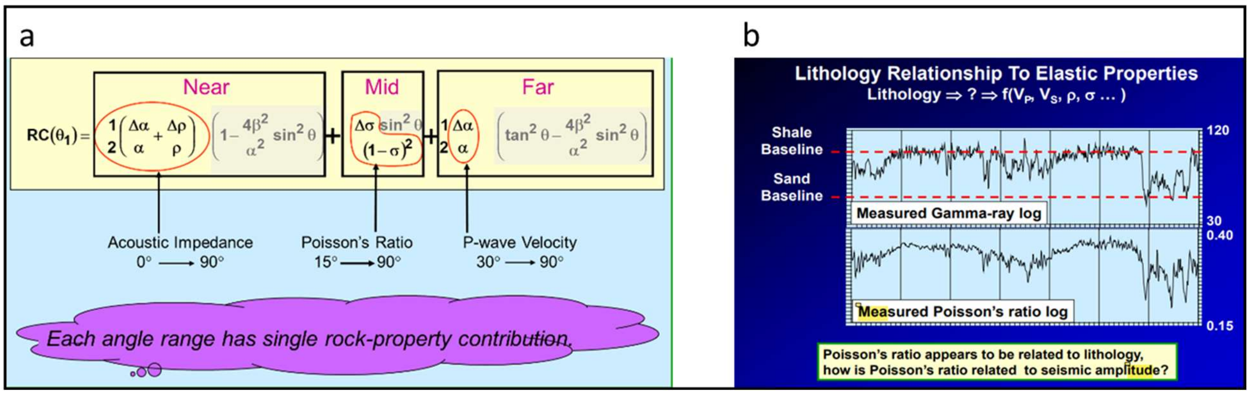

Figure 14. (a) Shuey three-part AVO equation. (b) Plot showing similarity between measured gamma ray curve and Poisson's ratio, establishing Poisson's ratio as the lithological rock indicator. (2001 SEG DISC, Hilterman, 2001)

Figure 15 shows a range limited PSTM well tie of the Togar 3D seismic survey, 0-600m offset-limited PSTM (left) and 1200-1800m offset-limited PSTM (right) with a conventional primary only synthetic seismogram. The 0-600m stacked seismic section ties the primary only synthetic seismogram effectively. The major reflectors with good S/N on the stack section were tied first and the amplitude and phase spectra were verified to prevent misties. Compared to the 0-600m stacked section, the far offset 1200-1800m stacked section contains extra reflections directly below the Murta and Namur formation tops. The reflection amplitude corresponds to a Class Two AVO anomaly (phase change) and reduces the correlation of the well tie.

To identify the source of the extra reflections in the 1200-1800m stacked section, the reflection response was modelled using the Shuey three-part AVO equation and Cooper Basin log information (Figure 16). In the AVO synthetic section (Figure 16), the offset distance and incidence angle ranges from 0-2080m and 0-60 degrees respectively. The contribution of the Poisson's ratio to the total reflectivity resides in the range from 15-90 degrees and 1100-1900m offset (red rectangle in the right portion of Figure 16). It is observable that reflections in the Poisson's reflectivity (ratio) range (red dashed box) corresponds to variable changes in the Poisson's ratio, cataloging these reflections to be lithostratigraphic.

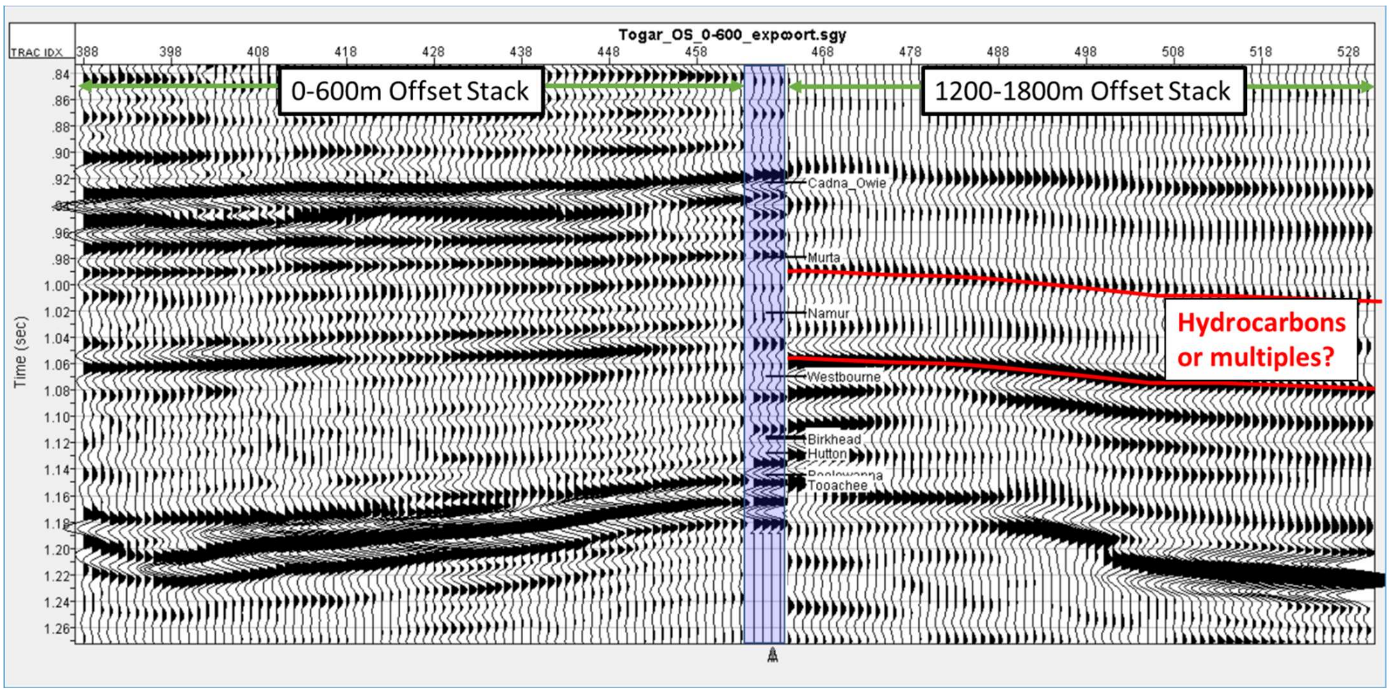

Figure 15. Togar 0-600m and 1200-1800m offset range well tie with a conventional primary only synthetic seismogram (adapted from Hilterman F. J, Seismic Amplitude Interpretation Course Notes, 2022).

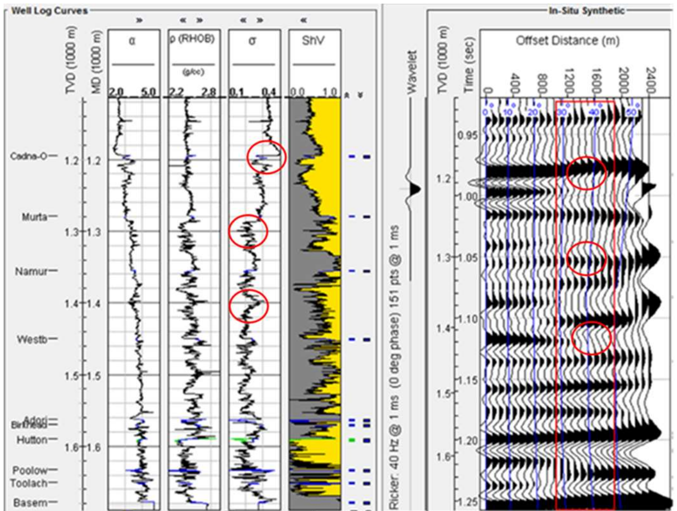

$$RC(\theta) \approx NI\cos^2\theta + 2.25\Delta\sigma\sin^2\theta + NI_{VEL}(\tan^2\theta - \sin^2\theta)$$

Figure 16. AVO synthetic section and the Shuey three-part AVO equation showing the Poisson's reflectivity range (adapted from Hilterman F. J, Seismic Amplitude Interpretation Course Notes, 2022).

Furthermore, the lithology in the AVO section was modified to contain only shale and to observe the reflection response for the Poisson's ratio range when there is no change in the lithology. When the lithology is changed, the Poisson's ratio needs to be recomputed. In Figure 17 you can observe the gently sloping trend of the Poisson's ratio in the well log, preventing any significant variations of the Poisson's reflectivity (which is the lithology indicator) in the well log. Apart from the stratigraphic marker, the reflections in the far offset range (1200-1800m) have been suppressed with an apparent increase in magnitude at the very far offsets, the P-wave velocity portion of the Shuey AVO equation.

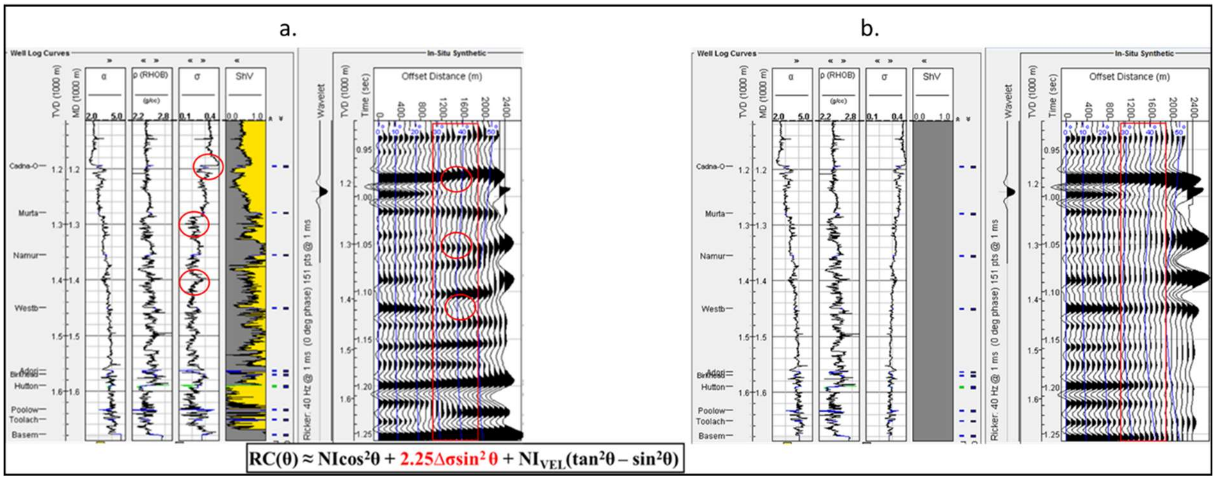

Figure 17. a. AVO synthetic section. b. AVO synthetic section with only shale lithology (modified from Hilterman F. J, Seismic Amplitude Interpretation Course Notes, 2022).

From the modelled AVO synthetic response, the extra reflections observed in the 1200m-1800m offset range stack correlate with variation in the Poisson's ratio, and lithostratigraphy of the study area, therefore these are lithostratigraphic reflections. Koefoed suggested the use of AVO to improve the quality of reflections on a seismogram by a sensible choice of distance from the shots to the seismograms. The invention of the synthetic seismograms led Hilterman (2001), to rearrange Koefoed's statement to, "Whenever a 1-D synthetic does not correlate with the field seismic, correlate the synthetic AVO response to the migrated CDP gathers at the well location". An AVO synthetic seismogram with offset range of 1100-1900m was generated and used to tie the 1200-1800m range limited stack section (Figure 18). The lithostratigraphic reflections in the Cooper basin are continuous and are easier to map than some of the chronostratigraphic reflections observed in the 0-600m near offset stack range. Lithostratigraphic reflections observed below the Murta and Namur formations appears on the AVO synthetic seismogram improving the correlation of the 1200-1800m offset stack range limited tie.

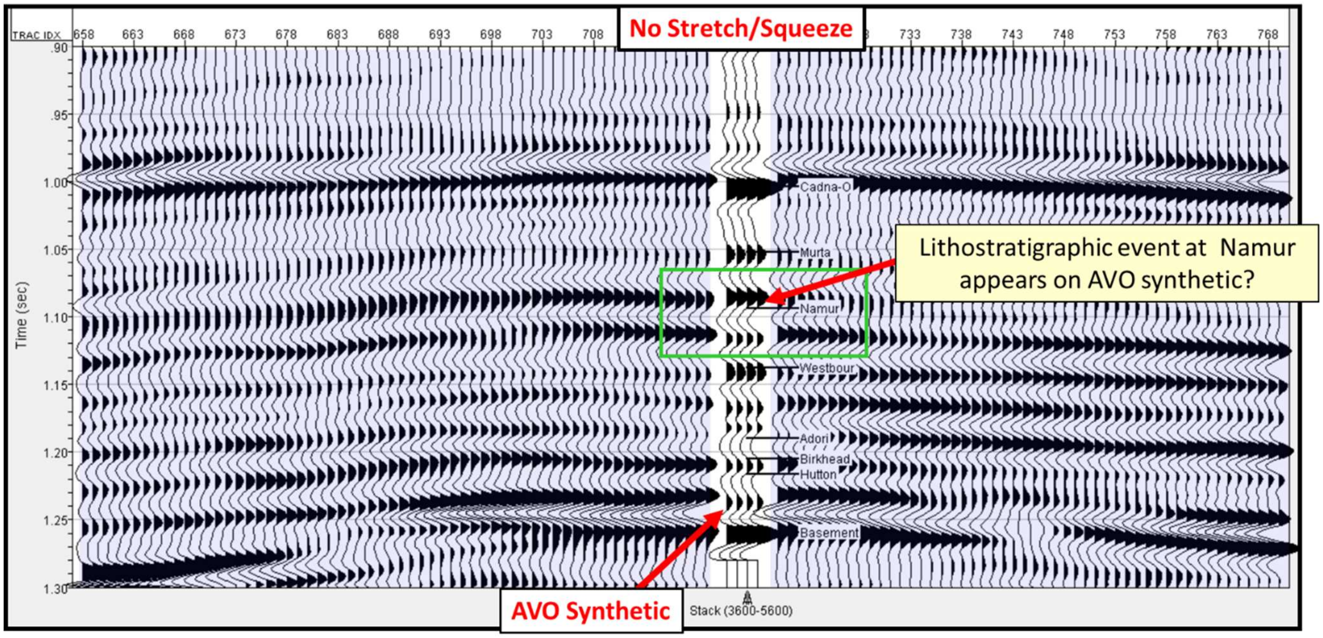

Figure 18. AVO synthetic well tie with the 1200-1800m range limited PSTM seismic image (adapted from Hilterman F. J, Seismic Amplitude Interpretation Course Notes, 2022).

VII. Cataloging misties

The quality of a well tie between the synthetic seismogram and the seismic image depends on the well log quality, seismic data processing quality, and the ability to extract a representative wavelet from the seismic data (Anderson et al, 2008). As discussed earlier, Figure 2 lists possible reasons for a mistie, cataloged into seismic, well-log quality and, theoretical model problems. By judiciously analyzing the various factors responsible for misties, the interpreter can carefully correct for or suppress these mechanisms and improve the quality of the seismic well tie and interpretation. Below are common reasons for misties which can be applied to other projects, especially where internal multiples are present.

A. Reasons for misties between synthetic and seismic

1. Wrong wavelet amplitude or phase spectra
2. Not tying good S/N reflectors first.
3. NI synthetic not tied to near-offset stack.
4. PSTM section ties AVO stack synthetic (lithostratigraphic reflectors)
5. Long-period multiples add extra events
6. Scattering attenuation and intrinsic attenuation make the synthetic shorter in time than the real seismic.
7. Shallow well log curves are not available to properly identify internal multiples
8. Well log curves not properly edited
9. Miscellaneous reasons (e.g., well location not correct, 2D sideswipe, limited areal extent of formation penetrated by well, etc)

VIII. Conclusion

Seismic well ties continue to be an active research topic due to its benefits in reservoir characterization and velocity modelling. Figure 2 from Hilterman 2001 and Section VII show various mechanisms responsible for misties and the necessity of investigating various components that go into the generation and interpretation of the seismic image and synthetic seismogram. In areas with severe stratigraphic filtering, it has been demonstrated that Hubral 1980's generalized primaries have been effective in the identification of long-and short-period internal multiples that degrade the seismic image and the quality of the synthetic seismogram. Low frequency source is required to maintain a higher S/N during transmission which can be quantified in the wavelet panel. The noise coda in a two-way transmitted wavelet is responsible for the extra events and often accounts for poor continuity below the evaporite bed sequence. After applying a low pass filter the long-period multiples are suppressed and the seismic image is improved, increasing the correlation of the well tie. Also, the use of a wavelet extracted from the seismic in the generation of the synthetic seismogram can aid to compensate for the delaying effect (similar to attenuation) of short-period internal multiples.

This study also demonstrates the value of theoretical models in the generation of the synthetic seismogram that improve the quality of the well tie. The amplitude variation with offset have been observed to reduce the correlation of a well tie. Lithostratigraphic reflections observed at far offsets in a Class Two AVO anomaly are generated due to the large variations in Poisson's ratio and provides better continuity for mapping reflection events. The AVO synthetic seismogram generated with the Shuey three-part equation separated the chronostratigraphic from the lithostratigraphic reflections in a CDP gather, and has been shown to effectively tie the seismic data at very far offsets.

Not discussed but needs to be remembered is the elastic impedance which is a generalization of the acoustic impedance for variable incidence angles. Elastic impedance has been demonstrated to provide a consistent and absolute framework to calibrate and invert nonzero-offset seismic data just as AI does for zero-offset data. With the elastic impedance there is the potential to improve the well tie are far offset stacks with a synthetic seismogram generated with the elastic impedance.

IX. Acknowledgements

I am grateful for the release of the seismic and well-log data by Dr Fred J. Hilterman and the permission to release this capstone research. I also want to thank Dr. Donald Van Nieuwenhuise and all the faculty in the university of Houston professional geophysics master's program that aided to my professional growth and understanding of the geophysical processes of the Earth.

X. References

- Anderson, P., and R. Newrick, 2008, Strange but true stories of synthetic seismograms. CSEG Recorder 33, 10.
- Goupillaud, P. L., 1961, An approach to inverse filtering of near-surface layer effects from seismic records: Geophysics, 26, 754–760, doi: 10 .1190/1.1438951.
- Hamilton M, J, 1962, A history of well logging. Geophysics, 27, 4, 507-527.
- Hilterman, F. J, 2001, Seismic amplitude interpretation. Society of Exploration Geophysicists- European Association of Geoscientists and Engineers.
- Hilterman, F. J., F. Nicholson, and C. Qi, 2018, Seismic interpretation when short-period internal multiples are present. The leading edge, 37, 1.
- Hilterman, F, J, 2022, Thin-Bed Transmission and Reflection Spectral Changes. Personal communication.
- Hilterman, F, J, 2022, Seismic Amplitude Interpretation Course notes. Personal communication.
- Hubral, P., S. Treitel, and P. R. Gutowski, 1980, A sum autoregressive formula for the reflection response. Geophysics, 45, 11.
- Hubral,P, 1983, Computing true amplitude reflections in a laterally inhomogeneous earth. Geophysics, 48, 8.
- Koefoed, O., 1955, On the effect of Poisson's ratio of rock strata on the reflection coefficient of plane waves: Geophys. Prosp., 3, 381-387.
- McDonal, F. J., R. L. Sengbush, and P. L. Lawrence, 1961, Interpretation of synthetic seismograms. Geophysics, 26, 2.

- O'Doherty, R. F., and Anstey. N. A.. 1971, Reflections on amplitudes: Geophys. Prosp., v. 19. p. 430-458.
- Ricker, N, 1953, The form and laws of propagation of seismic wavelets. Geophysics, 18, 1.
- Qi, C, and F. J. Hilterman, 2014, Quantification of signal and noise in twoway transmitted wavefields to improve well ties in Cooper Basin, Australia: Interpretation, 2, SD19–SD31, doi: 10.1190/INT-2013-01.
- Qi, C., 2016, Signal enhancement and impedance inversion for highly cyclically stratified sedimentation: PhD dissertation, University of Houston.
- Robinson, E. A., 1967, Multichannel time series analysis with digital computer programs: Holden-Day.
- Schoenberger, M, and F. K. Levin, 1974, Apparent attenuation due to intrabed multiples, Geophysics 39, 278–291.
- Shapiro, S. A., and P. Hubral, 1999, Elastic waves in random media: Fundamentals of seismic stratigraphic filtering: Springer.
- Sheriff definition of a seismic well tie. Encyclopedia dictionary.
- Stewart, R. R, and P. D. Huddleston, T. K. Kan, 1984, Seismic versus sonic velocities: A vertical seismic profiling study. Geophysics 49, 8, 27.
- Trorey, A. W, 1962, Theoretical seismograms with frequency and depth dependent absorption. Geophysics, 27, 6.
- Walden, A. T, and R. E. White, 1998 Seismic Wavelet Estimation: A Frequency Domain Solution to a Geophysical Noisy Input–Output Problem. 36, 1.
- White, R, E, and T. Hu, 1998, How accurate can a well tie be? The leading edge.
- Wuenschel, P. C, 1960 Seismogram synthesis including multiples and transmission coefficients. Geophysics XXV, 1.